Progress In Electromagnetics Research C, Vol. 84, 175–187, 2018

Design of Differential Source Fed Circularly Polarized Rectenna with Embedded Slots for Harmonics Suppression

Deepak Kumar* and Kalpana Chaudhary

Abstract—This work presents an enhanced rectenna with a differential source feeding scheme for radio frequency (RF) energy harvesting at 2.45 GHz frequency. A circularly polarized (CP) microstrip antenna with embedded slots is designed which efficiently attains harmonics suppression. By modifying size and position of two diametrically opposite triangular projections in the top patch, two orthogonal modes that have equal magnitude and are in phase quadrature are excited. The four radial slots embedded in the antenna can block 2nd and 3rd harmonics which is suitable for onboard rectenna design without harmonics filter. A microstrip tapered feed line is used to match antenna element with 50-ohm impedance. The designed antenna is then tested for RF energy harvesting in two ways. One is conventional single source fed rectenna (SSFR), and the other is proposed differential source fed rectenna (DSFR). In the DSFR, the designed antennas are differentially operated by making a difference of $\lambda g/2$ path length (λg Guided wavelength), and the ports are then connected to a differentially driven optimized rectifier circuit. For comparison, an SSFR and a DSFR are fabricated and tested. The circuit parameters in each case are optimized in Agilent Design System (ADS) 2011 software to maximize RF to direct current (DC) conversion efficiency. The proposed DSFR has a maximum efficiency (RF-DC) of 41.63% at 10 dBm RF input power. In the input power range from -20 dBm to 10 dBm, the DSFR has improved performance and higher efficiency over the SSFR.

1. INTRODUCTION

Over the last decade, satellite solar power station (SSPS) and wireless power transfer have become an interesting topic for the energy transmission in the future [1–4]. In wireless power transmission (WPT), the rectenna (antenna and rectifier) is a key element for receiving RF energy and converting RF energy into DC power [5]. For a conventional rectenna, the interface between antenna and rectifier circuit has a harmonic suppression filter which leads to circuit complexity and occupies extra space. Hence it is not suitable for compact rectenna design [6–8].

High frequency (HF) Schottky diodes are utilized for rectifying RF signal into DC power [9]. For low-level RF signal, the rectifier's efficiency is very poor. Thus energy harvesting may fail. A rectenna using differentially-fed rectifier for WPT has been proposed in [10], but it requires a differential antenna with coaxial probe feeding and a rectifier that is placed on a separate board. The rectenna device which is easy in fabrication and onboard integration with other components is highly preferable [11]. In another work, a differential rectenna scheme has been proposed in [12, 13] with improved efficiency at low signal level. However, the designed differential rectenna is linearly polarized and thus highly sensitive to the device or source movement. Therefore, an onboard CP rectenna with single microstrip feed is preferable for RF energy harvesting [14]. The Schottky diode rectifier has nonlinear property, and it produces signal harmonics when being connected to antenna [15]. Therefore, there is a requirement of the bandpass filter (BPF) between them to eliminate signal harmonics. A coaxial feed CP antenna

Received 14 February 2018, Accepted 9 May 2018, Scheduled 3 June 2018
* Corresponding author: Deepak Kumar (deepak.rs.eee14@itbhu.ac.in).
The authors are with the Department of Electrical Engineering, Indian Institute of Technology (BHU), Varanasi 221005, India.

with harmonics suppression capability has been proposed in [16]. Here, the patch with loaded slots provides higher-order resonance frequency shift which is different from operating frequency harmonics. Therefore, the proposed scheme eliminates the requirement of BPF; it is due to the mismatch of the signal harmonics and higher-order resonance mode. However, the proposed work is not suitable for compact rectenna application as it requires coaxial feed.

In this work, a new rectenna is provided with differential source feeding scheme for the low cost and efficient RF energy harvesting. First, a microstrip antenna with a diametrically opposite peripheral projection of isosceles right triangle shape which provides CP is designed. The antenna has four internal slots that are deliberately made to suppress higher order harmonics and enhance fundamental resonance mode. To show its harmonics rejection capacity, a conventional linearly polarized (LP) circular patch antenna without slots [16] is also designed and fabricated at 2.45 GHz, and their return loss results are compared. The performance of the proposed antenna is verified by the measurement results, such as radiation pattern and return loss. The designed antenna is then tested for RF energy harvesting in two ways. One is conventional SSFR, and the other is new DSFR. In the DSFR, the designed antennas are differentially operated by making a difference of $\lambda g/2$ path length, and the ports are then connected to a differentially driven optimized rectifier circuit. For comparison, an SSFR and a DSFR are fabricated and tested. The experimental results verify the performance of the proposed rectenna.

2. ANTENNA DESIGN

The geometry of the proposed antenna is shown in Figure 1. The substrate top conductor layer has a copper thickness 35 µm, a circular microstrip patch of radius R, and diametrically opposite peripheral projection of isosceles right triangle shape. The right angle triangular shape is selected to excite CP. Also, the top patch has four radial slots, with slot width Sw, and the gap between them is Sg. Slots are equidistance from the center with radial distance Rs. Here, slots are made purposely to block harmonic signals that are produced due to connection with the nonlinear load. The structure is designed on the substrate with length Ls and width Ws, and the bottom layer is covered with copper. The bottom conductor can work either as the RF ground or as the reflection plane. A tapered microstrip single feed is used to match antenna element with 50-ohm impedance at $w2$ as depicted in Figure 1.

The proposed antenna is designed on an FR4 substrate with thickness (h) 1.6 mm, dielectric constant (εr) 4.4, and loss tangent 0.02. The circular patch has two peripheral isosceles right triangle projection that is diametrically opposite at 45 degrees from the X-axis, and feed is connected at the

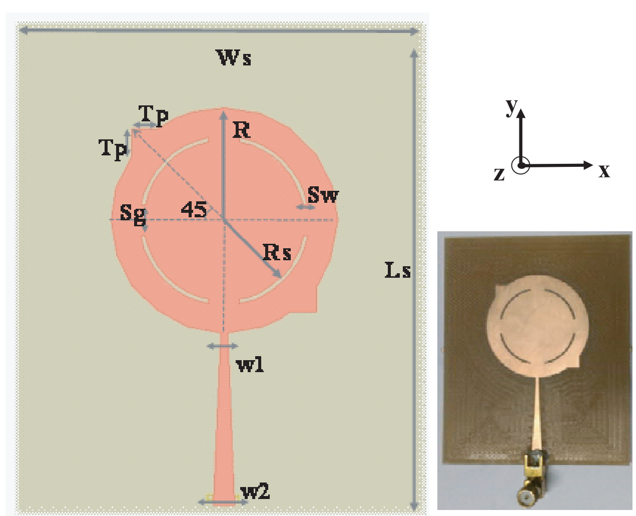

Figure 1. Geometry of proposed circular polarization antenna with harmonics suppression, the parameters (values in mm) are, $Ws = 60$, $Ls = 80$, $R = 16.3$, $Rs = 11.7$, $Tp = 4.1$, $Sw = 4$, $Sg = 4.5$, $W1 = 0.7$, $W2 = 3.02$.

lowest Y-axis point. This arrangement can excite the near-degenerate orthogonal resonant modes which provide CP. The isosceles right triangle projection has a dimension of length Tp. The antenna is simulated and designed in Agilent ADS 2011. The ADS has two solvers, by the methods of the moment and finite element method (FEM) solver. ADS FEM simulation has been used in this work.

2.1. Circular Polarization

To verify the CP behavior of the proposed antenna, the surface current distributions on the top patch at 2.45 GHz at 0°, 90°, 180°, and 270° are depicted in Figures 2(a), (b), (c), and (d), respectively. From these figures, one can easily predict that the surface current rotates synchronously with phase making it CP. At the desired resonant frequency, two orthogonal modes with the 90-degree phase difference for CP can be optimized by adjusting Tp size. It is also observed that if only one isosceles right triangle projection is used, left-hand circular polarization will be generated, and a diagonal mirror projection will generate right-hand circular polarization.

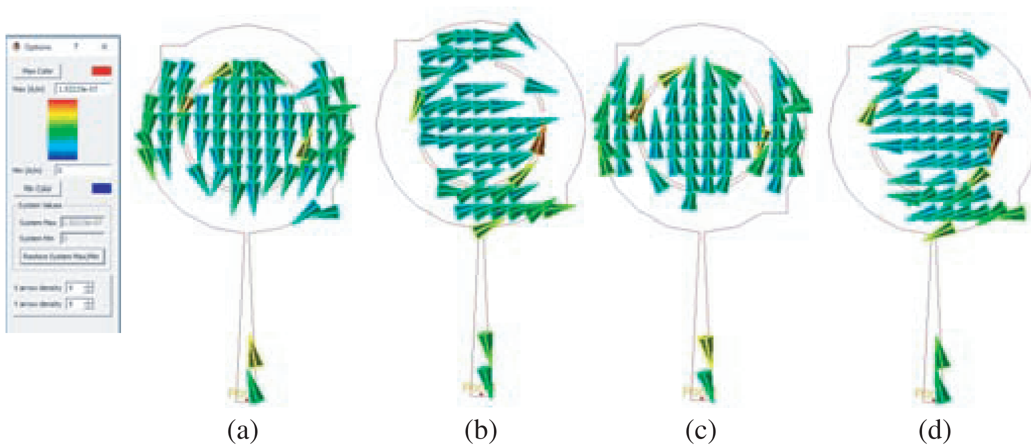

Figure 2. Surface current orientation at (a) 0, (b) 90, (c) 180, (d) 270 degrees, here degree means time progress in one period.

2.2. Harmonics Blocking

An antenna or any AC signal source when being connected with nonlinear elements produces signal harmonics; these harmonics can re-resonate antenna, and efficiency is highly reduced. Therefore, a BPF is required in-between to eliminate such undesired harmonics. However, there is an alternative which can also eliminate undesired harmonics without using a BPF. In this design, four radial slots in the patch are used instead of using BPF, and they have equidistance from the center. There are four equal gaps in between. The slots dimension and gap lengths are optimized or adjusted in such a way that fundamental mode of resonant is increased, but higher order resonant modes are reduced. The slots help to shift antenna's higher order resonant modes at different frequencies without disturbing its fundamental resonant mode. In this way, due to slots arrangement and optimization the operating frequency signal harmonics and antenna's higher order resonant modes are highly mismatched, and as a result, antenna's re-resonation and efficiency loss problem is eliminated. Thus a BPF can be removed.

The return loss for an LP circular patch antenna (without slots) has been compared with the proposed CP antenna (with slots); their simulated and measured return losses are shown in Figure 3. The LP circular patch antenna (without slots) has a fundamental resonant frequency at 2.45 GHz with a return loss of 14 dB. Its 2nd order resonance and 3rd order resonance are at 4.9 GHz (9.56 dB) and 7.35 GHz (14.6 dB), respectively. It is noticed here that higher-order resonant modes and signal harmonics are similar to the LP circular patch antenna, whereas the proposed CP antenna has an improved return loss of 37.2 dB at a fundamental resonant frequency, i.e., 2.45 GHz. However, its 2nd order resonance and 3rd order resonance are now shifted from 4.9 GHz to 4.75 GHz with 9.13 dB return loss and from 7.35 GHz to 6.75 GHz with 12.6 dB return loss, respectively. The proposed CP antenna's simulated return loss is decreased to 1.89 dB at 4.9 GHz and 2.31 dB at 7.35 GHz, and signal harmonics due to nonlinear elements are now suppressed. Figures 4(a), 4(b), 4(c) show the surface current densities of the proposed CP antenna resonances at fundamental, 2nd order and 3rd order, respectively. Due to embedded slots, higher order current paths have been increased, and higher order harmonics are now shifted to a different frequency. Here it is observed that variation of slot's radial distance, the gap between slots, and the higher-order mode current path can be adjusted, and it can be optimized as per the requirement.

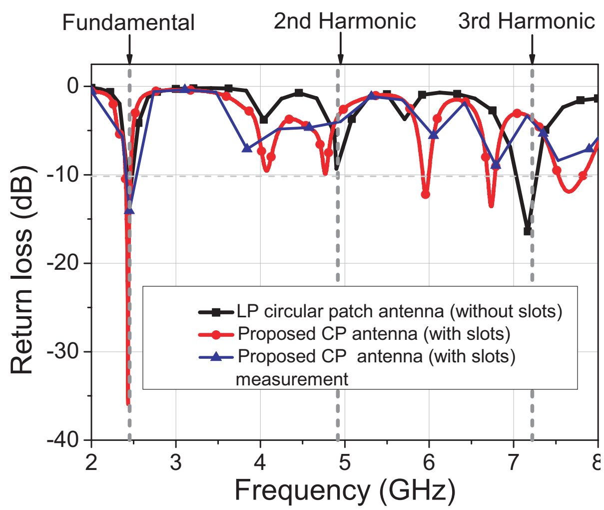

Figure 3. Simulated and measured return loss.

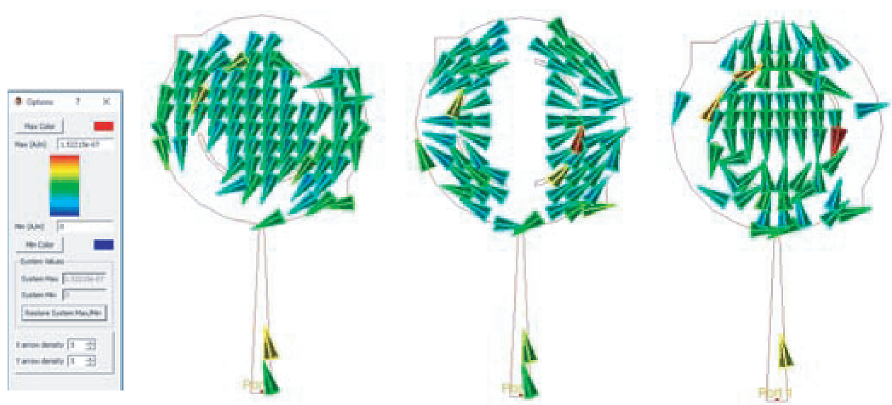

(a) (b) (c)

Figure 4. Surface current densities of the proposed antenna's resonance at (a) fundamental (2.45 GHz), (b) second order (4.75 GHz). (c) third order (6.75 GHz).

3. PARAMETRIC STUDY

Various parameters may influence the performance of the proposed antenna structure. The dimension of isosceles right triangle peripheral projection affects the circular polarization axial ratio bandwidth, and slots arrangement affects the higher order resonant mode. The parametric analysis is performed in Agilent ADS 2011 electromagnetic simulation to show their effects.

3.1. Effect of Isosceles Right Triangle Projection

In the FEM simulation, the isosceles right triangle projection diagonals Tp are varied from 3.6 mm to 4.2 mm. The return loss variation with different Tp is illustrated in Figure 5. Here with the increase in Tp size, the resonant frequency decreases, and the optimized value is obtained at 3.9 mm at which the structure has the highest CP axial ratio bandwidth and 2.45 GHz resonant frequency.

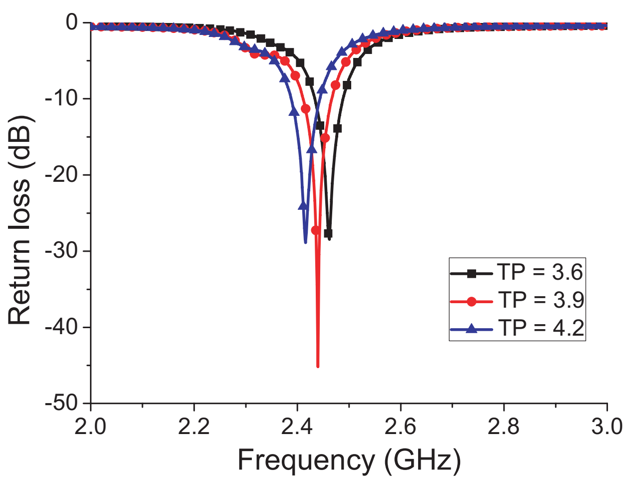

Figure 5. Simulation of proposed antenna with varying Tp (values in mm).

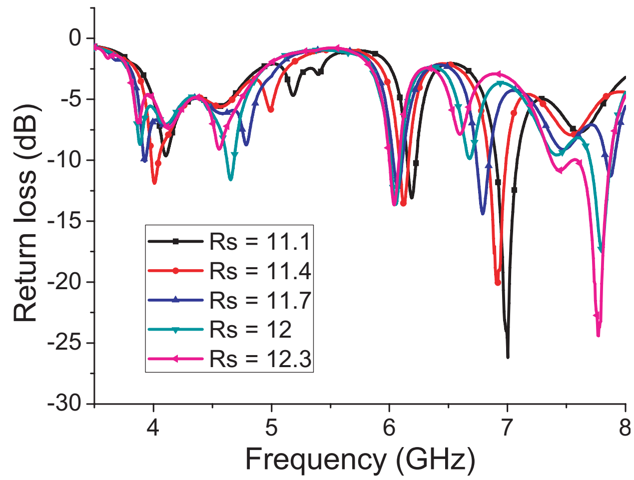

Figure 6. Simulation of proposed antenna with varying Rs (values in mm).

3.2. Effect of the Radial Slot

The radial slots distance from the center Rs is varied from 11.1 mm to 12.3 mm. The return loss variation with different Rs is shown in Figure 6. It is found that higher-order resonant modes depend on the Rs. Here resonant modes shift toward lower frequency while increasing the Rs. At the optimized Rs value, i.e., 11.7 mm, the antenna 2nd and 3rd resonant modes are shifted far below the nonlinear operating signal (2.45 GHz) harmonics.

3.3. Effect of Slot Gap

The radial slots have a gap between Sg; its value is varied from 3.3 mm to 4.5 mm as shown in Figure 7. The variation of Sg highly influences the higher-order resonant mode bandwidth. However, the lower bandwidth is preferred because there is a requirement to block nonlinear signal harmonics. The optimized value is found at Sg equal to 3.9 mm.

3.4. Results and Discussion

The prototype of the proposed antenna is designed, fabricated and tested to validate simulation results. Simulated and measured results show good agreement. The proposed antenna's measured return losses at 4.9 GHz and 7.35 GHz are 2.46 dB and 2.91 dB, respectively. Thus the proposed antenna effectively eliminates operating signal harmonics, and it can be connected to a nonlinear element without BPF. The radiation pattern in E-plane and H-plane is shown in Figure 8. The radiation patterns are identical in the two planes, confirming good circular polarization property. The antenna has a maximum gain of 3.16 dBi at the fundamental resonant frequency, i.e., 2.45 GHz. Simulated and measured axial ratios are shown in Figure 9. The circular polarization 3 dB axial ratio bandwidth is from 2.428 GHz to 2.459 GHz frequency that is found to be 31 MHz, with the minimum axial ratio of 0.68 dB.

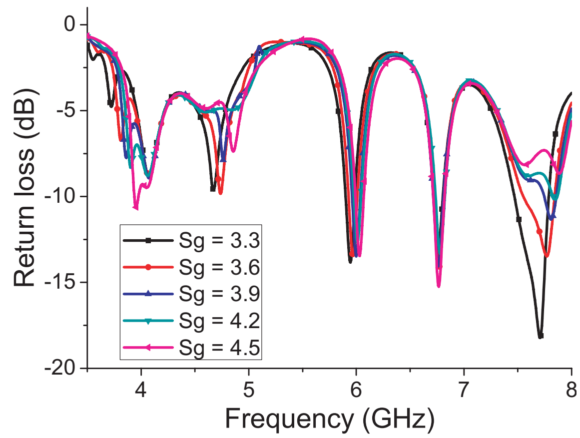

Figure 7. Simulation of proposed antenna with varying Sg (values in mm).

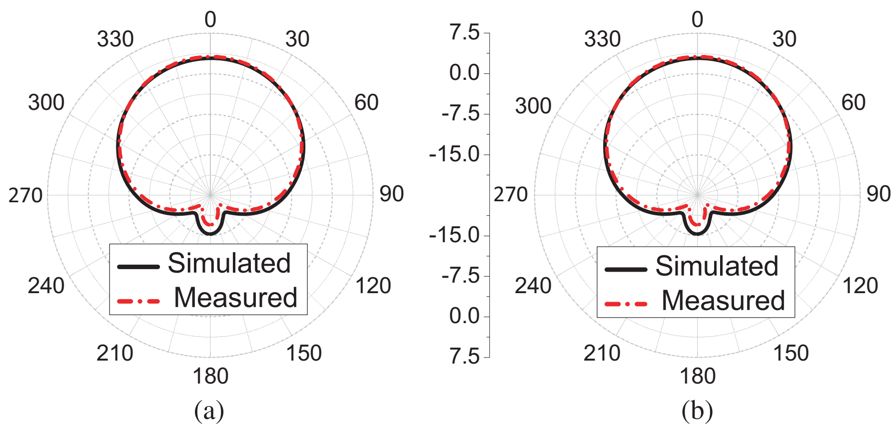

Figure 8. Simulated and measured radiation pattern of the proposed antenna. (a) E-plane. (b) H-plane.

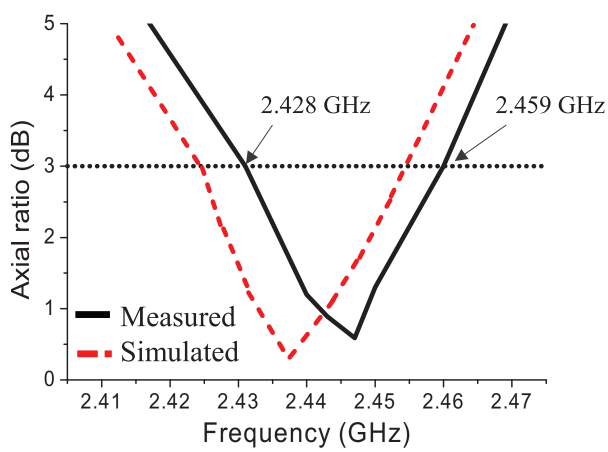

Figure 9. Simulated and measured axial ratio.

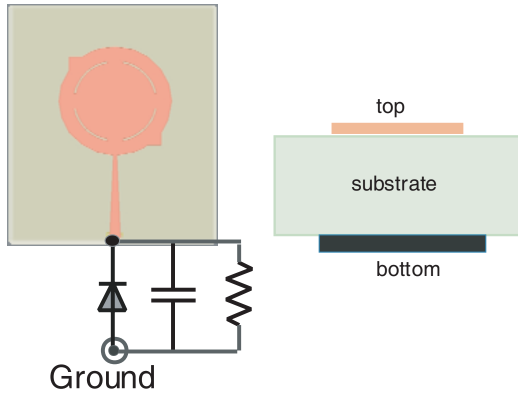

Figure 10. Single source antenna connected to a rectifier circuit.

4. RF ENERGY HARVESTING

4.1. SSFR

The configuration of conventional SSFR is shown in Figure 10. A single source antenna that is presented in Figure 1 has been used for RF energy harvesting. The rectifier with matching circuit is connected to the top microstrip feed at $w2$ and the ground. Here, the rectifier is designed on a separate board such that the RF-ground and DC-ground are isolated.

4.1.1. Single Driven Rectifier for SSRF

The single source antenna connected with rectifier circuit topology is shown in Figure 11. An RF source with P1 is applied here. In this circuit, inductor $L1$ and capacitor $C1$ act as a low-pass filter, while inductor $L2$ and capacitor $C2$ act as an output DC pass filter. Schottky diode HSMS-2860 (threshold voltage 350 mv & break down voltage 7 V) is used as D here. Circuit parameters $L1$, $C1$, $L2$, $C2$, and RL can be first calculated; then the software ADS can be utilized to optimize those parameters. This ADS OPTIM toolbox with proper optimization goal settings is used. Here optimization type genetic and iteration 500 is used. After optimization the parameters are $L1 = 7.5\,\mathrm{mH}$, $C1 = 0.37\,\mathrm{pF}$, $L2 = 7.88\,\mathrm{mH}$, $C2 = 280\,\mathrm{pF}$, and $RL = 200\,\mathrm{ohm}$. The circuit schematic of the proposed single driven rectifier with detailed parameters is provided in Figure 12.

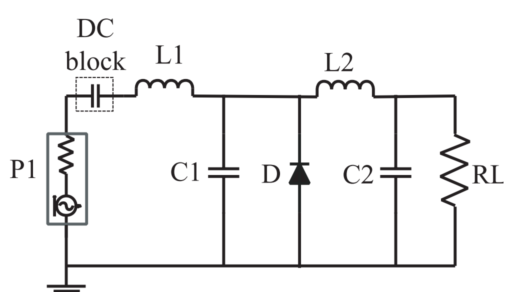

Figure 11. Circuit diagram of a single driven rectifier.

4.2. Proposed DSFR

Two top patches from Figure 1 are placed as in Figure 13(a), and differential input power is provided. For testing, this differential source is fed antenna in a real situation; a rat race coupler is used to transform two ports into a single port as shown in Figure 13(a). Here, a rat race coupler is designed in ADS at 2.45 GHz to provide differential power input, and the measured return loss of 14.6 dB is found

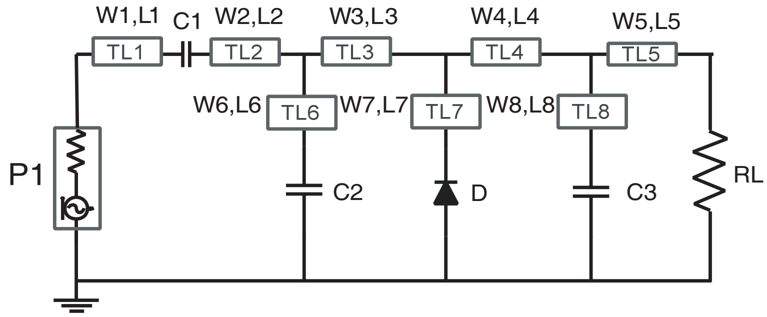

Figure 12. Circuit schematics of the proposed single-driven rectifier, the parameters are, $L1 = L2 = 2.5\,\text{mm}$, $L3 = 8.2\,\text{mm}$, $L4 = 8.2\,\text{mm}$, $L5 = 3\,\text{mm}$, $L6 = 7.1\,\text{mm}$, $L7 = 9.7\,\text{mm}$, $L8 = 7.4\,\text{mm}$ and $W1 = W2 = W3 = W4 = 1.12\,\text{mm}$, $W5 = 2.4\,\text{mm}$, $W6 = 5.1\,\text{mm}$, $W7 = 3.8\,\text{mm}$, $W8 = 3.5\,\text{mm}$, $C1 = 1\,\text{pF}$, $C2 = 4\,\text{pF}$, $C3 = 4\,\text{pF}$, $RL = 1200\,\text{ohm}$.

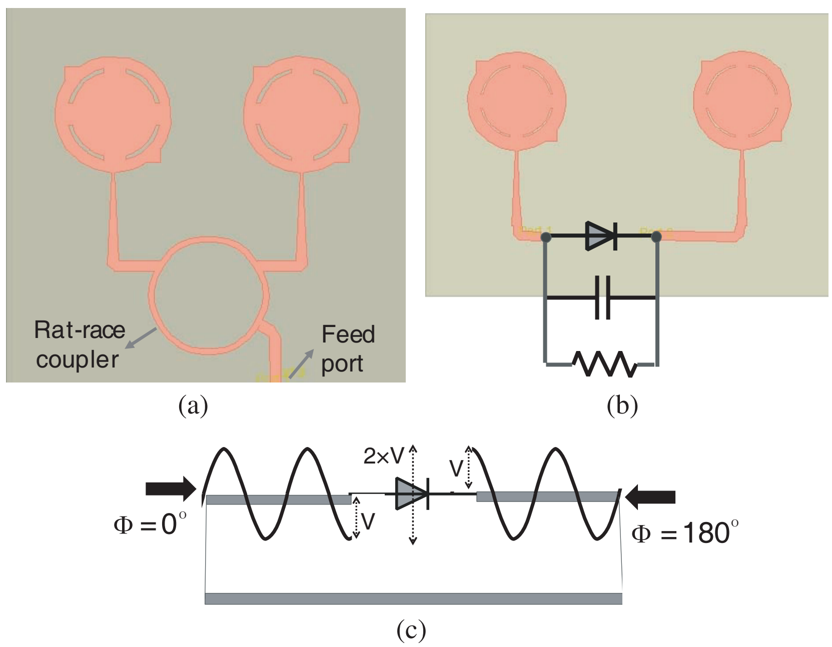

Figure 13. (a) Direct measurement of differential source fed antennas using rat race coupler to transform two ports into single port. (b) Differential source fed rectenna. (c) RF voltage applied to the diode in differential source fed condition.

at 2.45 GHz. In the differential structure with a rat-race coupler, two patches are symmetrical, and their feed lengths are equal. Now, the differential ports in Figure 13(a) are transformed into a single port. Thus the single driven rectifier that is designed for SSRF can be easily connected, and rectenna performance can be tested.

In this work, a DSFR configuration, which presented in Figure 13(b), is used. It is an alternate rectenna design without rat-race coupler, and it is also a compact design. Here two symmetrical patches from Figure 1 are used, but now their feed lengths have a path difference of $\lambda/2$ to provide differential source fed mode, and the port's connection is shown in Figure 13(b). At any instant, the voltage at port 1 and port 2 is 180° out of phase, because the two feeds have a path difference of length $L = 33.127\,\text{mm}$, i.e., $\lambda g/2$ (simulated and calculated at 2.45 GHz in ADS software). In this mode, the voltage applied to rectifier is shown in Figure 13(c). The geometry of the differential source fed rectenna is shown in Figure 14. In the construction, two proposed top patches from Figure 1 are connected as shown in Figure 14.

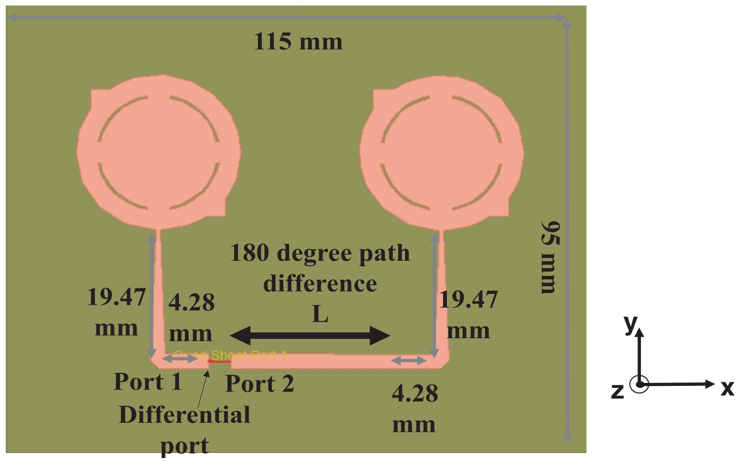

Figure 14. Differentially operated antenna.

4.2.1. Differentially Driven Rectifier for DSFR

The differentially driven rectifier topology for DSFR is shown in Figure 15(a). Here two sources (individual power $P1$) connected at two terminals are 180° out of phase. In this circuit, inductor $L3$ and capacitor $C3$ act as a low-pass filter, while inductor $L4$ and capacitor $C4$ act as a DC pass filter. The parameters $L3$, $C3$, $L4$, $C4$, and RL, can be first calculated; then the software ADS can be utilized to optimized those parameters with proper goal settings. Schottky diode HSMS-2860 is applied as D here. After optimization the parameters are $L3 = 16.17\,\text{mH}$, $C3 = 0.37\,\text{pF}$, $L4 = 22.28\,\text{mH}$, $C4 = 120\,\text{pF}$, and $RL = 200\,\text{ohm}$. The variation of differential driven rectifier's efficiency with different RL is plotted in Figure 16, and the variation of its output DC power with different RL is plotted in Figure 17. The circuit schematic of the proposed differentially driven rectifier with detailed parameters is provided in Figure 18.

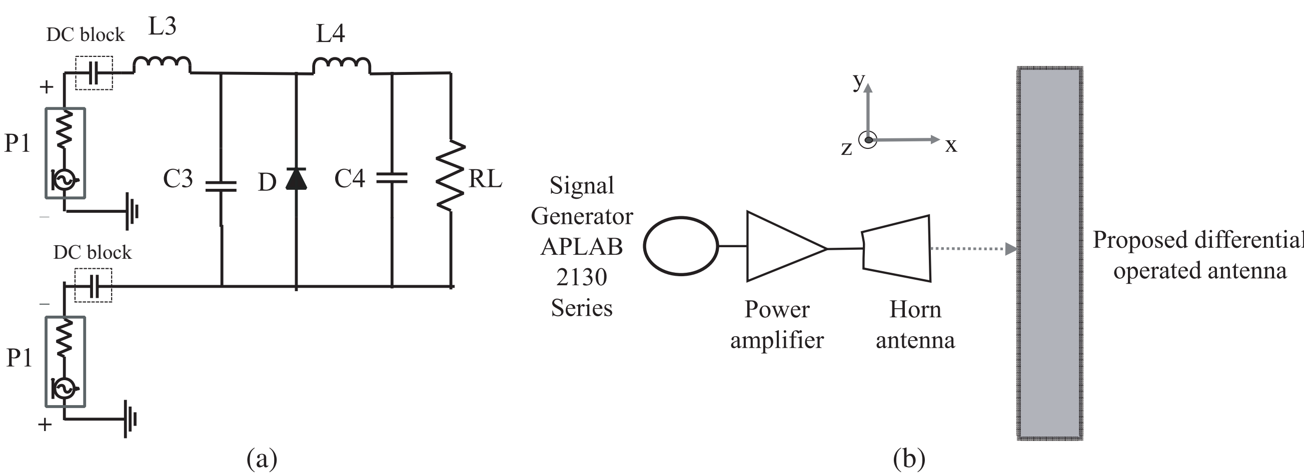

Figure 15. A differentially driven (a) rectifier schematic with (b) measurement setup.

4.3. Experimental Results

A DSFR using microstrip is designed and fabricated at 2.45 GHz. The circuit schematic and detailed parameters are shown in Figure 14 and Figure 18. For investigating the comparative performance, an SSFR is also fabricated and tested. Both rectennas are printed on an FR4 substrate, with height

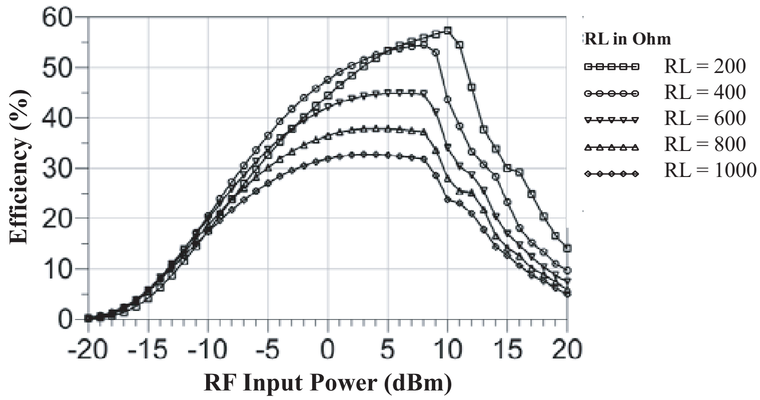

Figure 16. Variation of efficiency (%) with different RF input power (dBm), simulated results.

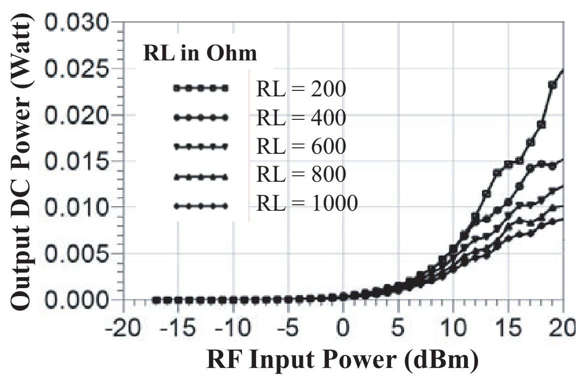

Figure 17. Variation of Output DC power (Watt) with different RF input power (dBm), simulated results.

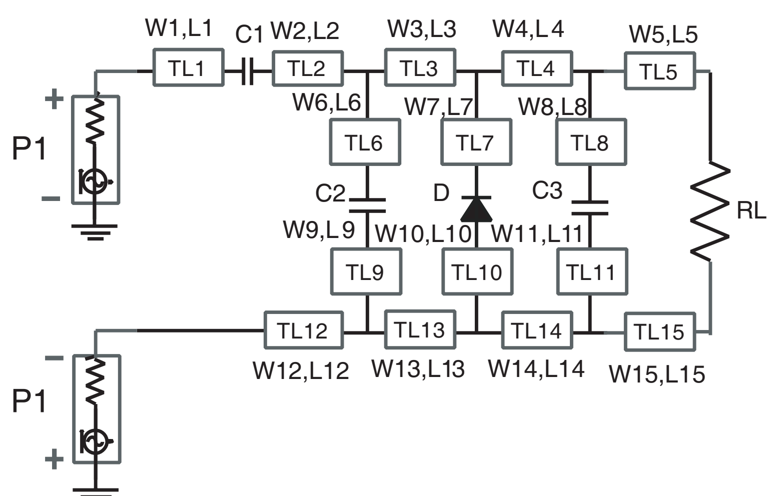

Figure 18. Circuit schematics of the proposed differentially driven rectifier, the parameters are, $W1 = W2 = W3 = W4 = W12 = W13 = W14 = 1.2\,\text{mm}$, $W5 = W15 = 3.4\,\text{mm}$, $W6 = W9 = 1.3\,\text{mm}$, $W7 = W10 = 3\,\text{mm}$, $W8 = W11 = 5.5\,\text{mm}$ and $L1 = 6.5\,\text{mm}$, $L2 = 4.5\,\text{mm}$, $L3 = L13 = 9.2\,\text{mm}$, $L4 = L14 = 10.2\,\text{mm}$, $L5 = L15 = 5.7\,\text{mm}$, $L6 = L9 = 4.9\,\text{mm}$, $L7 = L10 = 7.5\,\text{mm}$, $L8 = L11 = 4.9\,\text{mm}$, $C1 = 32\,\text{pF}$, $C2 = 91\,\text{pF}$, $C3 = 4\,\text{pF}$, $RL = 1800\,\text{ohm}$.

1.6 mm, dielectric constant 4.4 and loss tangent 0.02. In the measurement, RF-DC conversion efficiency can be calculated as

$$\eta\,(\%) = \frac{Output\ DC\ power}{RF\ Input} \times 100 \tag{1}$$

It is noticeable that in Equation (1), RF input for SSFR is ($P1$) while that for the DSFR is ($2 \times P1$).

For the SSFR and DSFR measurements, an APLAB 2130 Series Signal Generator with 9 kHz $\sim$ 3002 MHz frequency coverage with 50 Ohm VNA output port is used as RF source; it can excite RF power of 15 dBm. A high-directivity horn antenna (about 7 dBi gain at 2.45 GHz) is used, and it has larger dimension D 20 cm. Then the rectenna under test is placed at a distance of 70 cm from transmitting horn antenna. The distance in between satisfies far-field condition ($R > 2D^2/\lambda \sim 65$ cm) at 2.45 GHz, and the measurement setup is shown in Figure 15(b). The simulated and measured RF-DC conversion efficiencies of the two rectennas versus input power level are shown in Figure 19. In the input power range from -20 dBm to 10 dBm, the DSFR has significantly higher efficiency over the SSFR. The DSFR has a maximum efficiency of 41.63% at 10 dBm input power while the SSFR has a maximum efficiency of 37.88% at 14 dBm input power. It is noticeable here that due to polarization mismatch loss, the received powers of the SSFR and DSFR are decreased about 3 dB as both are CP rectennas. However, their efficiencies are stable irrespective of the rotation. A comparison among previous high-frequency rectifiers for energy harvesting application is also presented in Table 1.

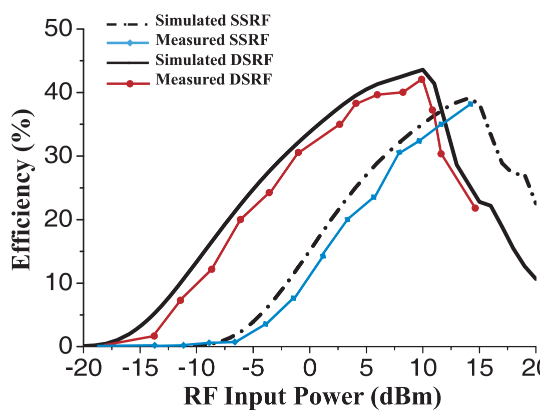

Figure 19. The simulated and measured efficiency of single fed and differentially fed rectenna.

Table 1. Comparison of previous high-frequency rectifiers for energy harvesting application.

Source	Operating frequency (GHz)	Feed type	Required RF power (mW) for maximum efficiency	Maximum measured efficiency (%)
[5]	0.9–1.9	(Coaxial feed)	3.16	23.5
[12]	5.8	(Microstrip feed)	10	23.3
[16]	2.4	(Coaxial feed)	2.5	51.5
This paper	2.45	(Microstrip tapered differential feed)	10	41.63 With 3 dB polarization mismatch loss

5. CONCLUSION

An efficient differential source fed CP rectenna is proposed and designed in this work. First, a circular patch antenna with a diametrically opposite peripheral projection of isosceles right triangle shape for circular polarization has been designed. It has internal radial slots for harmonics suppression up to third order that is suitable for rectifier connection for RF energy harvesting. The 2nd and 3rd harmonics return losses are suppressed to 2.46 and 2.91, respectively, thus BPF can be eliminated. For RF energy harvesting, the proposed differential source antenna is connected with a differentially driven rectifier to perform higher efficiency and yields larger output power than the single source driven rectenna. In the DSFR, the RF-DC conversion efficiency reaches 41.63% at 10 dBm while the SSFR has a maximum efficiency of 37.88% at 14 dBm. Also in the input power range from −20 dBm to 10 dBm, DFSR has higher efficiency than SSFR. Therefore, this low profile rectenna strategy is suitable for cost-effective highly efficient and onboard rectenna for RF energy harvesting application.

ACKNOWLEDGMENT

We would like to thank all concerned with the Indian Institute of Technology (BHU) Varanasi for their all-out effort to support us in completing this research.

REFERENCES

1. Takhedmit, H., et al., "Efficient 2.45 GHz rectenna design including harmonic rejecting rectifier device," *Electron. Lett.*, Vol. 46, No. 12, 811, 2010.
2. Chaudhary, K. and B. R. Vishvakarma, "Feasibility study of LEO, GEO and Molniya Orbit based satellite solar power station for some identified sites in India," *Adv. Sp. Res.*, Vol. 46, No. 9, 1177–1183, 2010.
3. Shinohara, N. and H. Matsumoto, "Design of Space Solar Power System (SSPS) with phase and amplitude controlled magnetron," *Asia-pacific Radio Science Conference*, 624–626, 2004.
4. Shinohara, N. and H. Matsumoto, "Microwave power transmission system with phase and amplitude controlled magnetrons," *Proceedings of 2nd International Conference on Recent Advances in Space Technologies (RAST 2005)*, 28–33, 2004.
5. Jabbar, H., S. Member, Y. S. S. Member, and T. T. Jeong, "RF energy harvesting system and circuits for charging of mobile devices," *IEEE Trans. Consum. Electron.*, Vol. 56, No. 1, 247–253, 2010.
6. Sun, H., Y. X. Guo, M. He, and Z. Zhong, "Design of a high-efficiency 2.45-GHz rectenna for low-input-power energy harvesting," *IEEE Antennas Wirel. Propag. Lett.*, Vol. 11, 929–932, 2012.
7. Lu, J.-H. and S.-C. Lin, "Broadband design of planar circularly polarized annular-ring antenna for RFID applications," *Progress In Electromagnetics Research Letters*, Vol. 68, 1–8, 2017.
8. Prakash, K. C., S. Mathew, R. Anitha, P. V. Vinesh, M. P. Jayakrishnan, P. Mohanan, and K. Vasudevan, "Circularly polarized dodecagonal patch antenna with polygonal slot for RFID applications," *Progress In Electromagnetics Research C*, Vol. 61, 9–15, 2016.
9. Douyere, A., J. D. L. S. Luk, and F. Alicalapa, "High efficiency microwave rectenna circuit: Modelling and design," *Electron. Lett.*, Vol. 44, No. 24, 1–2, 2008.
10. Sun, H., "An enhanced rectenna using differentially-fed rectifier for wireless power transmission," *IEEE Antennas Wirel. Propag. Lett.*, Vol. 15, 32–35, 2016.
11. Chin, C. H. K., Q. Xue, and C. H. Chan, "Design of a 5.8-GHz rectenna incorporating a new patch antenna," *IEEE Antennas Wirel. Propag. Lett.*, Vol. 4, No. 1, 175–178, 2005.
12. Matsunaga, T., E. Nishiyama, I. Toyoda, and A. Structure, "5.8-GHz stacked differential mode rectenna suitable for large-scale rectenna arrays," *IEEE Trans. Antennas Propag.*, Vol. 63, No. 12, 5944–5949, 2015.

13. Sakamoto, T., Y. Ushijima, E. Nishiyama, M. Aikawa, and I. Toyoda, "5.8-GHz series/parallel connected rectenna array using expandable differential rectenna units," *IEEE Trans. Antennas Propag.*, Vol. 61, No. 9, 4872–4875, Sep. 2013.
14. Chou, J. H., D. B. Lin, K. L. Weng, and H. J. Li, "All polarization receiving rectenna with harmonic rejection property for wireless power transmission," *IEEE Trans. Antennas Propag.*, Vol. 62, No. 10, 5242–5249, 2014.
15. Ren, Y. J. and K. Chang, "5.8-GHz circularly polarized dual-diode rectenna and rectenna array for microwave power transmission," *IEEE Trans. Microw. Theory Tech.*, Vol. 54, No. 4, 1495–1502, 2006.
16. Huang, F.-J., T.-C. Yo, C.-M. Lee, and C.-H. Luo, "Design of circular polarization antenna with harmonic suppression for rectenna application," *IEEE Antennas Wirel. Propag. Lett.*, Vol. 11, 592–595, 2012.